

Article

# Study on the Mechanism of Stress Sensitivity Changes in Ultra-Deep Carbonate Reservoirs

Wanjie Cai <sup>1,2</sup>, Shan Jiang <sup>1,2,\*</sup> and Hong Liu <sup>3</sup><sup>1</sup> College of Geoscience, Yangtze University, Wuhan 430100, China; 2021710421@yangtzeu.edu.cn<sup>2</sup> Key Laboratory of Exploration Technologies for Oil and Gas Resources, Ministry of Education, Yangtze University, Wuhan 430100, China<sup>3</sup> School of Science, East China University of Technology, Nanchang 330000, China; llhh81@163.com

\* Correspondence: jiangshan0712@126.com

**Abstract:** Quantitative evaluation of stress sensitivity of ultra-deep carbonate reservoirs has been one of the challenges in exploration and development, and the problem of permeability loss law in ultra-deep carbonates under variable stress conditions has not been solved so far and further research is urgently needed. Through experimental and numerical simulation methods, the stress-sensitive evaluation equations were established based on matrix-type carbonate and fractured carbonate reservoirs, the stress-sensitive changes under different Young's modulus were discussed, and the degree of permeability loss under different stresses was evaluated. Finally, the dual-media model of ultra-deep carbonate was established, and the practical application was carried out in the Shunbei area of the Tarim Basin. Studies have shown that (1) under the same effective stress, the stress sensitivity of matrix-type and fracture-type carbonate reservoirs is related to the Young's modulus of the rock skeleton. In matrix-type carbonate reservoirs, rocks with a larger Young's modulus have smaller rigidity and stronger stress sensitivity. In fracture-type carbonate reservoirs, the stress sensitivity is relatively weak under a smaller Young's modulus, and relatively strong under a larger Young's modulus. (2) Measured under the conditions of 87 MPa of peripheral pressure, 50 MPa of flow pressure, and 120 °C, the effective stress of matrix-type carbonate reservoirs has an exponential relationship with the permeability of reservoirs. The degree of stress sensitivity for fracture-type is generally higher than that of matrix-type reservoirs, and the smaller the Young's modulus, the larger the difference in stress sensitivity. (3) The stress sensitivity of typical ultra-deep carbonates in the Shunbei area of the Tarim Basin is higher by establishing a dual-porosity model based on the initiating pressure gradient, which supports new evidence for the characteristics of ultra-deep carbonates with high-stress sensitivity. In actual production, the impact of stress sensitivity on the reservoir volume calculation and efficient development of ultra-deep carbonate reservoirs requires critical attention.



**Citation:** Cai, W.; Jiang, S.; Liu, H. Study on the Mechanism of Stress Sensitivity Changes in Ultra-Deep Carbonate Reservoirs. *Appl. Sci.* **2024**, *14*, 2322. <https://doi.org/10.3390/app14062322>

Academic Editor: Nikolaos Koukoulas

Received: 29 January 2024

Revised: 5 March 2024

Accepted: 8 March 2024

Published: 9 March 2024



**Copyright:** © 2024 by the authors. Licensee MDPI, Basel, Switzerland. This article is an open access article distributed under the terms and conditions of the Creative Commons Attribution (CC BY) license (<https://creativecommons.org/licenses/by/4.0/>).

**Keywords:** stress-sensitive; ultra-deep carbonate reservoirs; dual-porosity model; Tarim Basin

## 1. Introduction

Since 2000, China has been exploring ultra-deep (with a depth of burial over 6000 m) carbonate reservoirs [1]. According to data from the China National Petroleum Corporation (CNPC), as of the end of 2021 [2], China has identified oil and gas reserves of more than 100 billion barrels in ultra-deep carbonate reservoirs, of which the oil and gas resource-rich areas are mainly concentrated in the Tarim Basin, Sichuan Basin, and Ordos Basin [3–5]. With the continuous advancement of exploration and extraction technology, the exploration and development capabilities of ultra-deep carbonate reservoirs have been significantly improved [6–9]. The vast reserves of oil and gas in ultra-deep carbonate reservoirs can provide important support for China's future energy supply.

Ultra-deep carbonate reservoirs are complex storage media for oil and gas, with highly heterogeneous reservoirs and complex spatial structures [10]. During the extraction process,

as the remaining reserves continuously decrease, the underground pressures gradually decrease, causing the deformation of the rock skeleton. The increasing effective stress causes the reservoir's internal pore structure to deform, along with the formation of micro-fractures and changes in the mechanical properties of rocks [11]. The effective stress to which it is subjected increases, causing the deformation of the internal pore structure of the reservoir, micro-fractures and other deformations, and ultimately the phenomenon of the loss of permeability and decline in production capacity, which is also known as the stress sensitivity of carbonate rock. The stress sensitivity of carbonate reservoirs not only affects the reserve evaluation in the development of carbonate oil and gas fields, but also has important implications for the formulation of development technology indicators for carbonate oil and gas fields. First, the stress sensitivity of carbonate reservoirs directly affects the size of the storage space, which in turn affects the calculation of the true reserve of oil and gas reservoirs by petroleum engineers during the development process. In addition, with the deepening of the exploitation degree, the stress sensitivity of the carbonate reservoir will directly change the pore structure of the reservoir, which will affect the process of oil and gas seepage and influence the final development effect. Therefore, stress-sensitive parameters are important parameters that affect the oilfield development process. Therefore, how to scientifically and accurately evaluate the stress sensitivity of carbonate reservoirs has become a difficult problem in the research of carbonate reservoirs.

Researchers have conducted extensive research on the stress sensitivity of reservoirs; Jones [12] conducted stress sensitivity experiments on fractured carbonate reservoirs. By measuring the permeability of core samples at different confining pressures, Jones [12] found that there is a linear relationship between rock confining pressure and permeability. An empirical formula was derived from the experimental data; Pedrosa [13] successfully solved the flow equations of the system considering stress sensitivity, and Kikani [14] made further improvements based on Pedrosa's work. Tong Dengke [15] analytically studied the effect of stress sensitivity on reservoir permeability in oil reservoir flow problems and defined the stress parameter alpha. They also analyzed several typical pressure curve graphs using numerical simulation methods. Li Chuanliang [16] defined the stress sensitivity index as the percentage loss of reservoir properties when the formation pressure drops a certain value. They derived the stress sensitivity index from the relationship between effective stress and the rate of permeability loss.

Numerous scholars have conducted laboratory experiments to study the relationship between reservoir permeability and effective stress [17–20]. They have investigated the impact of different reservoir characteristics, such as confining pressure, rock type, and the degree of fracturing on rock sample permeability. As a result, several theoretical models have been established, including the binomial model, power function model, and exponential model. Common theoretical equations for calculating the relationship between reservoir permeability and effective stress include the following:

$$K = K_{ref} * (\sigma_{re} / \sigma_{ref})^{-\alpha} \quad (1)$$

$$K = K_{ref} * e^{-\beta * (\sigma_{re} - \sigma_{ref})} \quad (2)$$

$$K = m * \sigma_{re}^2 + g * \sigma_{re} + z \quad (3)$$

where,  $\sigma_{re}$  is the effective stress, in MPa;  $\sigma_{ref}$  is the reference effective stress, in MPa;  $K$  is the permeability, in mD;  $K_{ref}$  is the permeability under the reference effective stress ( $\sigma_{ref}$ ), in mD;  $\alpha$  is the stress sensitivity coefficient of the power law model;  $\beta$  is the stress sensitivity coefficient of the exponential model; and  $g$  and  $z$  are fitting coefficients.

Most scholars currently research the stress sensitivity of reservoirs based on conventional sandstone reservoirs or theoretical discussions without specific geological conditions. However, research on the stress sensitivity of ultra-deep carbonate reservoirs is relatively less in-depth. Therefore, this study aims to quantitatively study the stress sensitivity of fracture-porosity reservoirs in ultra-deep carbonate reservoirs. This study will be based

on numerical simulations and the rock mechanic characteristics of carbonate reservoirs to calculate the relationship between reservoir permeability and effective stress in the Shunbei oilfield fault zone of the Tarim Basin. This research will provide crucial guidance for developing and adjusting oilfield development plans.

## 2. Stress-Sensitive Modelling of Ultra-Deep Carbonate Reservoirs

Based on the characteristics of carbonate reservoirs and the influence of the mechanical parameters of rocks (such as Young's modulus and Poisson's ratio) under different stresses, quantitative evaluation formulas for the stress sensitivity of matrix-type and fracture-type carbonate reservoirs were derived using the classical mechanics solution by Griffith, Darcy's law [21,22].

The matrix-type carbonate reservoir is a significant type of rock that contains both oil and gas resources. To evaluate this reservoir quantitatively, we must consider its petrophysical properties as well as its mechanical parameters, such as permeability, porosity, and Young's modulus. These factors primarily affect the stress sensitivity of the reservoir. A formula has been developed to reflect the stress sensitivity of the matrix-type carbonate reservoir, which considers changes in permeability, increases in porosity, and changes in Young's modulus under different stresses.

The fractures carbonates reservoir is a complicated structure made up of matrix-type carbonate reservoirs and a series of fractures. A formula for evaluating stress sensitivity has been developed, which takes into account the permeability, number, and size of fractures under different stress conditions. This formula can guide the development and stability of intensive exploited fracture systems under various stress levels, and effective exploitation and development can be achieved in carbonate fracture-type reservoirs.

These quantified evaluation formulas provide theoretical support and practical references for the evaluation and management of carbonate reservoirs and their oil and gas resources under different stress conditions.

### 2.1. Derivation of Equations for Stress Sensitivity Evaluation of Matrix-Type Carbonate Reservoir

The change mechanism of stress sensitivity in matrix-type carbonate reservoirs is through the changes in the internal pore structure and skeletal structure of the rock. When the rock is subjected to stress, the internal pore structure of the rock tends to close, resulting in a reduction in porosity and permeability, which lowers the flow capacity of the reservoir. Additionally, the skeletal structure of carbonate reservoirs is relatively weak and undergoes plastic deformation under stress. It can cause a reduction in the volume of the rock and induce uncontrollable factors such as reservoir fracturing and crack formation [23].

Therefore, a physical experiment using true core samples was carried out to study the stress sensitivity of the ultra-deep carbonate matrix by the mentioned factors.

Note:

1. The samples were collected from ultra-deep carbonate samples of the Northwest Bureau of SINOPEC.
2. This study focuses on ultra-deep carbonate reservoirs that are deeply buried and difficult to obtain core samples from. During the sampling process, the cores were severely damaged. Therefore, we selected two relatively intact cores as representatives in this study, and the specific sample parameters can be found in Table 1.

**Table 1.** Basic parameters of the samples.

Core Number	Diameter/mm	Permeability/mD	Porosity/%
A1	69.246	0.032	0.1306
A2	54.228	0.133	0.1528

This experiment involved two test samples, sequentially numbered A1 and A2. The experiment was conducted under conditions of a confining pressure of 87 MPa, a temper-

ature of 120 °C, and nitrogen as the fluid medium. By maintaining a constant confining pressure on the core samples, changes in flow pressure were used to alter the effective stress experienced by the cores.

Experimental Procedure:

1. Measure the permeability and porosity of the samples before any loss occurs;
2. Place the core samples into the core holder and initialize the core permeability tester;
3. Ensure that the confining pressure remains constant and changes the flow pressure to 10 MPa, 15 MPa, 20 MPa, 25 MPa, 30 MPa, 35 MPa, 40 MPa, 45 MPa, and 50 MPa. After each pressure point stabilizes, measure the permeability of the rock sample and calculate the permeability loss rate;
4. After all pressure-point tests are completed, turn off the equipment;
5. Replace the core and repeat the aforementioned operations (Figure 1).

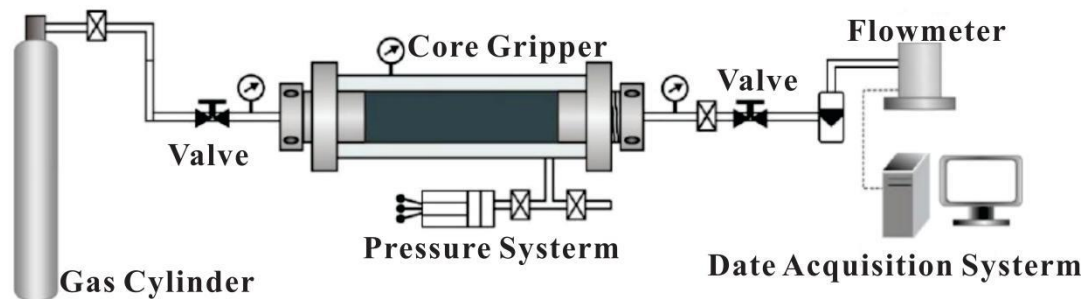


**Figure 1.** Stress sensitivity experimental equipment.

The value of  $K_0$  is the original permeability of the formation, and  $K_h$  is the permeability measured under different fluid pressures that correspond to different effective stresses. Based on the data obtained in the high-temperature and high-pressure testing conditions (Tables 2 and 3), the permeability–effective stress relationship curve (Figure 2) and permeability loss rate ( $K_h/K_0$ )–effective stress relationship curve (Figure 3) were drawn.

**Table 2.** Core A1 stress sensitivity experimental data.

Core Number	Porosity/%	Confining Pressure/MPa	Flow Pressure/MPa	Permeability/mD	Rate of Change in Permeability/%
A1	0.1306	87	65	0.0541	0.0
		87	60	0.0453	16.4
		87	50	0.0352	34.9
		87	45	0.0318	41.3
		87	40	0.0305	43.7
		87	35	0.0273	49.5
		87	30	0.0255	53.0
		87	25	0.0239	55.9
		87	20	0.0215	60.3
		87	15	0.0213	60.6
		87	10	0.0189	65.1
		87	5	0.0185	65.8

Table 3. Core A2 stress sensitivity experimental data.

Core Number	Porosity/%	Confining Pressure/MPa	Flow Pressure/MPa	Permeability/mD	Rate of Change in Permeability/%
A2	0.1528	87	65	0.174	0.0
		87	60	0.154	11.2
		87	50	0.142	18.1
		87	45	0.133	23.7
		87	40	0.123	29.4
		87	35	0.120	30.9
		87	30	0.120	31.1
		87	25	0.114	34.7
		87	20	0.112	35.6
		87	15	0.113	35.0
		87	10	0.109	37.5
		87	5	0.105	39.6

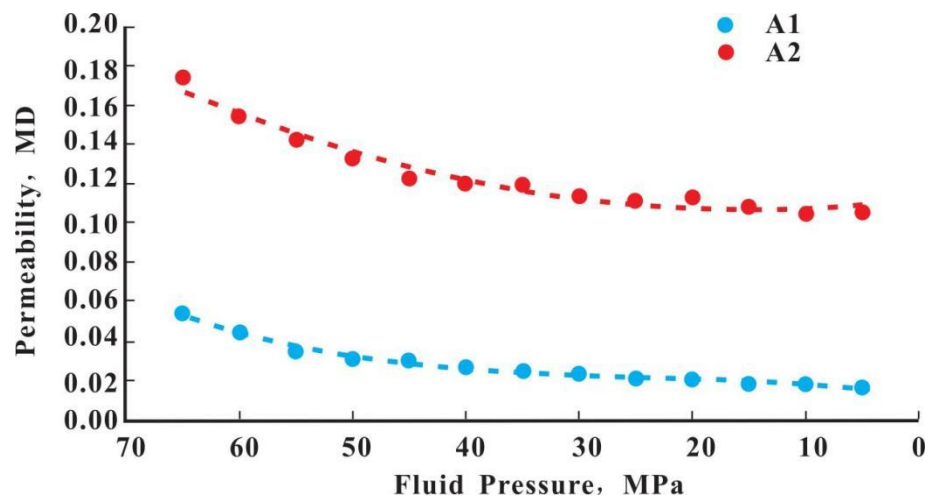


Figure 2. Depletion-type permeability change curve.

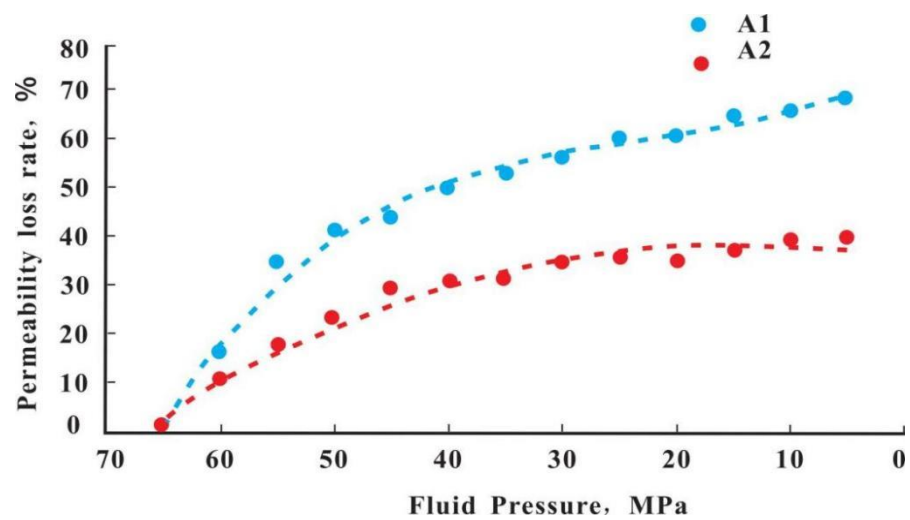


Figure 3. Depletion permeability-loss-rate curve.

The results of the stress sensitivity experiment show that the permeability decreases as the effective stress increases. However, the degree of permeability loss and recovery characteristics of different rock samples vary greatly with changes in formation pressure. According to the impact of the stress sensitivity coefficient and permeability loss rate on the stress sensitivity under experimental conditions, a fitting model is established based on the experimental data to establish the relationship between the effective stress coefficient, Young's modulus of matrix-type carbonate rock, and permeability. The relationship between these parameters can be described as follows:

$$K = K_0 * e^{-(\alpha_E)\sigma} \quad (4)$$

where  $\sigma$  is the effective stress of the rock, MPa;  $K_0$  is the rock permeability at stress 0, mD;  $K$  is the rock permeability with effective stress  $\sigma$ , mD; and  $b$  is the stress sensitivity constant of the rock, no dimension.

The relationship between permeability and Young's modulus in terms of the effective stress coefficient ( $\alpha$ ) at different levels of permeability can be expressed by the following equation based on experimental data:

$$\alpha_E = 1.465 - 0.324 \ln E \quad (5)$$

The relationship between rock sample permeability and effective stress is derived based on experimental data processing:

$$K = K_0 * e^{-0.009324\alpha_E(\sigma-\sigma_0)} \quad (6)$$

where  $K$  is the permeability affected by stress sensitivity, mD;  $K_0$  is the original permeability, mD;  $\sigma$  is the effective stress, MPa; and  $\sigma_0$  is the initial effective stress, MPa.

## 2.2. Derivation of Stress-Sensitive Formulae for Fractured Carbonates

In the field of geology and rock mechanics, fractures can be classified based on different modes of crack propagation, known as Mode I, Mode II, and Mode III fractures [24,25]. These modes are associated with different types of stress conditions and deformation mechanisms, and they can affect the behavior and stability of rocks differently. Here is a brief explanation of each mode:

**Mode I fracture (opening mode):** Mode I fractures occur when a crack propagates perpendicular to the direction of the applied tensile stress. This is commonly referred to as an opening-mode fracture, where the crack surfaces move away from each other. Mode I fractures are typically associated with tensile loading and are important in rock fragmentation and tension-induced failures.

**Mode II fracture (sliding mode):** Mode II fractures occur when a crack propagates parallel to the direction of the applied shear stress. This mode is characterized by sliding along the plane of the crack surfaces. Mode II fractures are associated with shear loading and can occur in situations where rocks are subjected to lateral or sliding forces.

**Mode III fracture (tearing mode):** Mode III fractures occur when a crack propagates perpendicular to the direction of the applied tearing stress. In this mode, the crack surfaces slide past each other and move parallel to the direction of the applied stress. Mode III fractures are less common in geological contexts but can be important in certain types of underground mining or faulting events.

In ultra-deep carbonate reservoirs, fractures play a dominant role in the loss of formation pressure, exacerbating the stress sensitivity effect of the reservoir [26–30]. Through numerical simulations comparing the effects of factors, such as the magnitude of Young's modulus, Poisson's ratio, and the fracture dip angle on the permeability loss of ultra-deep carbonate reservoir-rich formations, the role of fractures in stress sensitivity could be determined.

It was found that reservoirs with developed fractures were more stress-sensitive than those without fractures. Fracture density and dip angle were observed to significantly impact stress sensitivity. Therefore, it is important to factor in the impacts of fractures and corresponding stress sensitivity effects during exploration and development of ultradeep carbonate reservoirs, and to take appropriate measures to maximize reservoir development effectiveness.

Taking into account the abundant development of fractures in carbonate reservoirs, stress sensitivity can usually be described by introducing a stress sensitivity coefficient of permeability using Poiseuille and Darcy's laws as a basis for derivation. Therefore, based on Young's modulus and Poisson's ratio, a three-parameter numerical simulation model based on Young's modulus, Poisson's ratio, and effective stress is typically used to calculate the relationship between effective stress and permeability. This method enables a systematic description of stress sensitivity in carbonate reservoirs, and it can provide a solid foundation for further studies of stress sensitivity and corresponding adjustments to oil and gas reservoir monitoring, development, and exploration processes.

The general form of Darcy's law is as follows:

$$Q = K * A * \frac{\Delta P}{\mu L} \quad (7)$$

where  $Q$  is the flow rate of fluid per unit time,  $m^3$ ;  $K$  represents permeability, mD;  $A$  is the cross-sectional area perpendicular to the flow direction,  $m^2$ ;  $\Delta P$  is the pressure difference driving fluid flow, MPa;  $\mu$  represents fluid viscosity,  $m^2/s$ ; and  $L$  is the fluid flow distance, m.

Poiseuille's equation is as follows:

$$Q_s = \frac{\pi}{4\mu} * \frac{\Delta P}{L} * \frac{a^3 * b^3}{a^2 + b^2} \quad (8)$$

where  $Q_s$  is the total flow rate through the crack,  $m^3$ ;  $\mu$  is the fluid viscosity,  $m^2/s$ ;  $a$  and  $b$  are the dimensions of the short and long axes in the plane of the crack, respectively; and  $\Delta P$  is the pressure difference in the flow direction.

Young's modulus based on rocks defines the relationship between stress and strain. Young's modulus (also called elastic modulus) refers to the unit strain of a material under a certain stress, usually represented by the symbol  $E$ :

$$E = \frac{\Delta P}{\varepsilon} \quad (9)$$

$$\varepsilon = \frac{\Delta L}{L_0} \quad (10)$$

where  $E$  represents Young's modulus of the rock,  $\varepsilon$  represents the linear strain of the rock, and  $\Delta P$  represents the effective stress.  $L$  represents the change in length of the crack, and  $L_0$  represents the original length of the crack.

The relationship between permeability and effective stress can be expressed as

$$K = K_0 * e^{-\alpha * \varepsilon} \quad (11)$$

where  $K$  is the reservoir's permeability, mD;  $K_0$  is the initial permeability, mD; and  $\alpha$  is the stress sensitivity coefficient.

Substituting (9) and (10) into (11), the permeability and effective stress can be rewritten as

$$K = K_0 * e^{-\alpha * (\frac{\Delta P}{E})} \quad (12)$$

### 3. Influence of Different Young's Modulus on Stress Sensitivity

#### 3.1. Matrix-Type Carbonate Reservoirs

For matrix-type carbonate reservoirs with a high Young's modulus, the rock has relatively low rigidity and is more susceptible to both elastic and plastic deformation. When subjected to increased stress, plastic deformation of the rock matrix may occur, leading to pore closure and deformation, thereby affecting permeability. Therefore, matrix-type carbonate reservoirs with a high Young's modulus exhibit a higher degree of stress sensitivity.

For matrix-type carbonate reservoirs with a low Young's modulus, the rock has relatively higher rigidity and is less susceptible to plastic deformation. When subjected to increased stress, the rock matrix may undergo limited deformation, but that of pore closure and deformation are relatively small and insignificant, leading to minor changes in permeability. Therefore, intragranular matrix-dominated carbonate reservoirs with a low Young's modulus exhibit relatively low stress sensitivity. If the Young's modulus  $E$  of these rocks is changed to 10~30 GPa, the stress sensitivity curve would exhibit characteristics as shown in Figure 4.

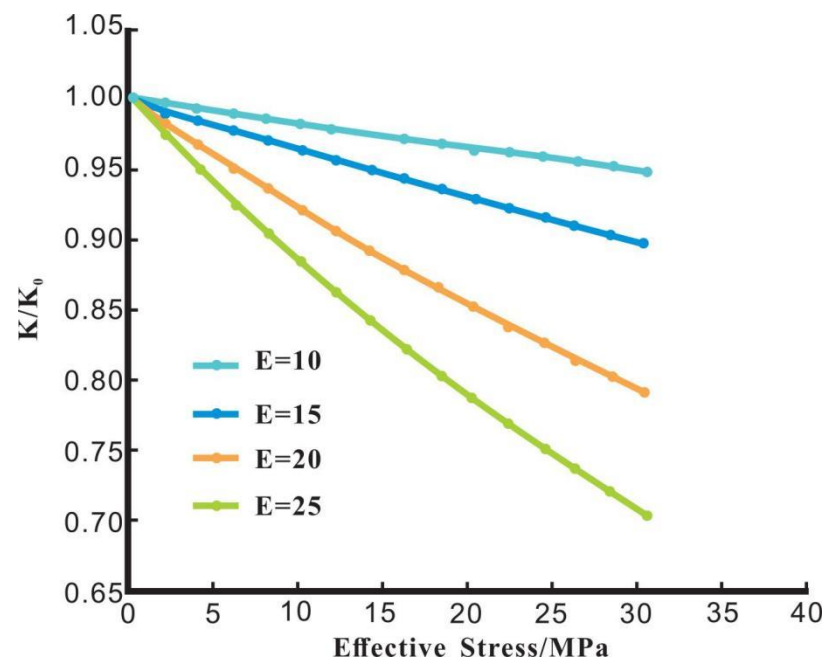


Figure 4. Stress sensitivity curve of matrix-type carbonate rock under variable Young's moduli.

In general, the stress sensitivity of matrix-type carbonate reservoirs is relatively low, when compared to other types of rocks. As the Young's modulus increases, the rate of permeability decrease gradually intensifies. The maximum loss of permeability is less than 4%. Furthermore, the stress sensitivity of intragranular matrix-dominated carbonate reservoirs uniformly decreases with increasing Young's modulus. This indicates that the higher the Young's modulus of the rock, the greater the rock's stiffness, and the smaller the effect of external stress on it. As a consequence, the rock's stress sensitivity weakens.

#### 3.2. Fractured Carbonate Reservoirs

For fractured carbonate reservoirs, fractures are present within the rock itself, compromising its integrity. When external stress is applied to the rock, the fractures may expand or close due to variations in stress. The sensitivity of fractured carbonate reservoirs to stress changes varies according to Young's modulus of the rock.

Fractured carbonate reservoirs with a low Young's modulus possess higher elastic deformation capability, and fractures tend to close relatively easily without significant deformation. Thus, for fractured carbonate reservoirs under these circumstances, their

stress sensitivity may be low. However, in fractured carbonate reservoirs with a high Young's modulus, the rock stiffness is greater, and external stress changes tend to cause the widening of the already existing fracture(s). At this point, the stress sensitivity of fractured carbonate reservoirs may generate high sensitivity, expressing that the rock is highly sensitive to variations in stress. It should be noted that the stress sensitivity of fractured carbonate reservoirs is also influenced by other factors, such as the number, size, and distribution of fractures. In addition, the actual rock properties and technical conditions can also impact stress sensitivity. If the Young's modulus  $E$  of these rocks is changed to 10~30 GPa, the stress sensitivity curve would exhibit characteristics as shown in Figure 5.

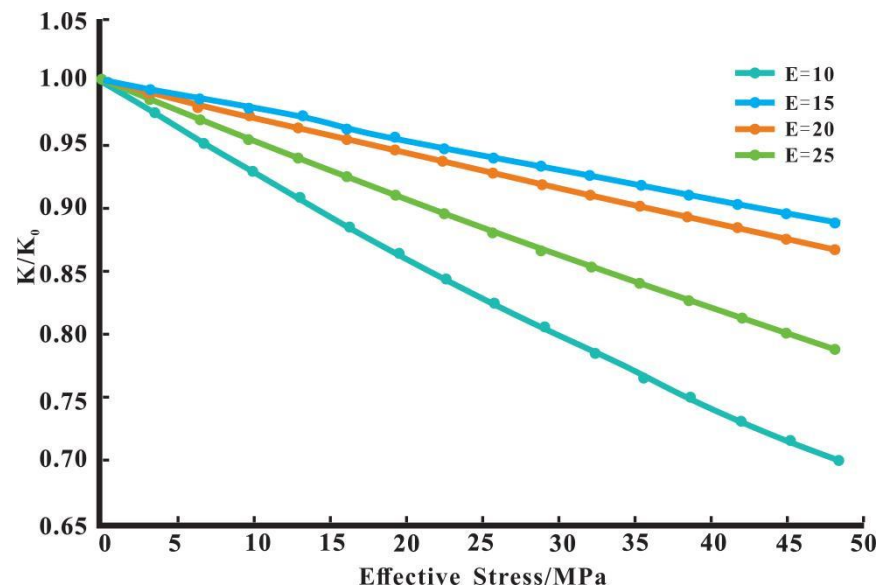


**Figure 5.** Stress sensitivity curve of fractured carbonate rock under variable Young's moduli.

Overall, fractured carbonate reservoirs exhibit significantly higher stress sensitivity than matrix-type carbonate reservoirs. With increasing Young's modulus, the rate of permeability decrease due to external stress varies; its stress sensitivity uniformly decreases. This demonstrates that the stiffness of the fractured carbonate reservoirs increases vis-a-vis their Young's modulus; i.e., with increasing Young's modulus, the sensitivity to stress changes reduces. Fractured carbonate reservoirs with a high Young's modulus can increase the rock's stiffness, resulting in decreased permeability decline in response to changes in external stress.

#### 4. Example Application

We have chosen the ultra-deep carbonate reservoirs of the T74 formation in the Shunbei area of the Tarim Basin for studying the stress sensitivity of ultra-deep carbonate reservoirs. The Tarim Basin is currently situated in the southern part of China's Xinjiang Uygur Autonomous Region. This area features broken seam cavernous ultra-deep carbonate reservoirs spanning from the eastern foothills of the Pamir Plateau in the west to the Rob Lake depression in the east, and extending from the southern foot of the Tianshan Mountains in the north to the northern foot of the Kunlun Mountains in the south [31–33]. As China's largest inland basin, the tectonic region is located between the Tianshan Mountain range and Kunlun mountain range with abundant Permian slope-deposition-environment hydrocarbon source rocks in the northern and eastern parts of the basin, where the upper stratum is home to together complete life-storage-cover geological amounts [34]. Movement by multiple fault planes serves as favorable conditions for oil and gas migration and accumulation, leading to highly optimal capture conditions. Due to the influence of the fault zone, and the matrix in the reservoir serving as the primary storage unit, the fractures

acting as the main fluid flow channel demonstrate strong reservoir heterogeneity and the fractures heavily impact the stress sensitivity of the reservoir.

Phase 1: Middle Cambrian. This stage was the main period of formation for strike-slip fault systems within the craton. Due to the collision between the West Kunlun and Tarim blocks, the study area underwent a regional uplift leading to the formation of several compressional uplifts and small-scale regional fault systems. Phase 2: Late-middle to early-late Cambrian. This stage saw the main period of activity for the strike-slip fault system under strong compression. In the Silurian and Devonian periods, a shallow en echelon-style strike-slip fault developed due to the deep-seated fault zone. Phase 3: Late Devonian to Indosinian. During this stage, the study area was mainly affected by the compressive force of the South Tian Shan Mountains, and the strike-slip fault zone continued to be active. The deep-seated faults formed in the early stages of this period were also reactivated. Additionally, small-scale faults developed in the Carboniferous and Permian in the Shunbei area. Phase 4: Yanshan to Himalayan. This stage was the period of evolution for the Tarim Basin depression where the study area had undergone fracturing activities due to tensional stress. In the early stage, NE-trending strike-slip faults were active, while their activity diminished in the late stage, leading to the final formation of strike-slip faults in the Shunbei area.

In the early stages, the northeast-trending strike-slip faults were very active. In the later stages, their activity gradually decreased, eventually leading to the formation of strike-slip faults and pattern II fractures in the Shunbei area (Table 4).

**Table 4.** Fracture statistics.

Depth	Type of Fracture	Fracture Length		Fracture Width		Number	Densities
		Corridor	Average	Corridor	Average		
7358–7527	Natural fractures	70–1470	365	0.1–20	2.1	70	0.41
7527–7581	Natural fractures	70–300	127	0.03–0.3	0.09	8	0.15
7581–7751	Natural fractures	40–530	221	0.02–2	1.1	48	0.28
7550–8163	induced fractures	180–520	281	0.3–6	1.1	26	0.04

The development of natural fractures in the study area was investigated through resistivity logging. Resistivity logging is relatively sensitive to fracture identification and can be affected by factors, such as fracture orientation, extension length, and mud invasion depth. In lateral logging, because the measuring circuit is in parallel with the low-resistance fracture, the resistivity is greatly affected in the vertical fracture segment and can be identified by the lateral logging for vertical fractures. In the induction logging, the measuring circuit is in parallel with the horizontal fracture, and the resistivity is greatly affected in the horizontal fracture segment such that it can identify vertical fractures.

According to previous research, when high-angle fractures develop, lateral resistivity displays a positive anomaly while middle and low-angle fractures display a negative anomaly or a low-resistivity peak (Figure 6). At present, the overall tectonic stress field in the southern section of the fault zone is oriented in a northeast–north direction, and there is an obvious deviation in the local stress field, with the direction of the Earth’s stress being near east–west and north–northeast (Figure 7). Therefore, in this study, DFN discrete modeling and dual media numerical simulation were used to simulate the impact of stress sensitivity in the stratigraphic layer. In the numerical simulation process, the dual media model divided the matrix and fractures into two systems, and the reservoir permeation occurred in the fractures. Different formulas for stress sensitivity were assigned to the matrix and fractures, respectively, to calculate the change in permeability under the influence of stress sensitivity.

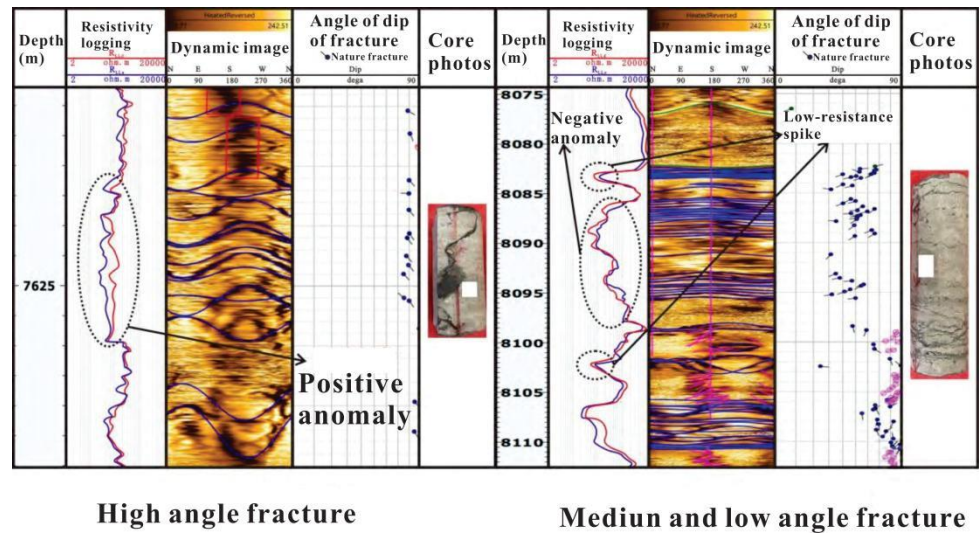


Figure 6. Characteristics of the resistivity difference display.

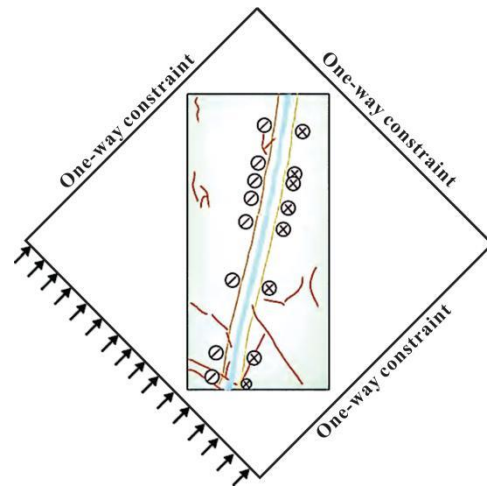


Figure 7. Structural stress field-simulated boundary conditions.

4.1. Establishment of Dual-Porosity Model

Considering the strong heterogeneity of the reservoir, the fluid flow behavior, and the current development status, we determine the parameters of the carbonate reservoir model (Table 5). The size of the established model is 1680 m × 756 m × 900 m with the grid dimensions of 15 m × 2 m × 10 m.

Table 5. Parameters for the dual-porosity model in the simulator.

Model Attribute	Value	Model Attribute	Value
Matrix model grid	NX = 112 NY = 378 NZ = 90	Fracture model grid	NX = 112 NY = 378 NZ = 90
Model geometry	160 m * 756 m * 900 m	Model grid step size	DX = 15 DY = 2 DZ = 10
Mean matrix permeability	37.613 mD	Mean fracture permeability	152.818 mD
Mean matrix porosity	18.92%	Mean fracture porosity	1.092%
Middle depth of reservoir	6743 m	Matrix fracture conductivity	Tr = CDARCY * K * V * σ
Reservoir pressure	87.75 MPa	Matrix to fracture cross-flow coefficient	σ = 4(1/lx <sup>2</sup> + 1/ly <sup>2</sup> + 1/lz <sup>2</sup> )

For the equations in Table 5, CDARCY is the Darcy constant; K is the rock permeability; V is the matrix volume per rock unit; lx is the distance between fractures in the X direction; ly is the distance between fractures in the Y direction; and lz is the distance between fractures in the Z direction.

According to the mechanical parameters of rock samples (Table 6), Young's modulus of the matrix rock is 53.41 GPa and Poisson's ratio is 0.201, and Young's modulus of the fracture is 5.041 GPa and Poisson's ratio of the fracture is 0.33. According to the stress deformation method of the matrix-fracture dual-media model, the change in core porosity and permeability loss caused by effective stress is

$$K = K_0 * e^{-0.125 * (\frac{\Delta P}{5.041})} \quad (13)$$

**Table 6.** Table of rock mechanical parameters.

Parameters	Value	Parameters	Value
Maximum horizontal principal stress	0.024 MPa	Young's modulus of the matrix	53.41 GPa
Minimum horizontal principal stress	0.0181 MPa	matrix Poisson's ratio	0.201
Vertical principal stress	0.025 MPa	Uniaxial compressive strength of matrix	96.98 MPa
Formation porosity pressure	0.011 MPa	Young's modulus of the fracture	5.041 GPa
Direction of maximum horizontal principal stress	NE 43.8°	Fracture Poisson's ratio	0.33
The Biot coefficient	1	Direction of cracks	44.1°

When the effective stress  $\Delta P$  is 0,  $K = K_0$ , i.e., no stress sensitivity occurs, which is realistic. For rock samples in the same state, at this time with the increase in effective stress, the reservoir permeability loss occurs, and the smaller the Young's modulus, the greater the difference in stress sensitivity.

Due to the presence of an underlying aquifer, which supplies the energy lost from the production process, the current model has adopted the use of the initiation of pressure gradients to limit this energy supply and maintain balance during the production process. This allows for the better control of fluid movement between adjacent layers through the creation of a minimum pressure difference between neighboring lower-pressure layers. By maintaining this pressure gradient within the threshold specified by Table 7, one can limit any lateral movements between the cells and help calibrate the minimum boundary pressure for initiating these pressure gradients within the simulated volume. This method could also be used to study the changes in production indicators as a result of various pressure gradients initiated between different zones. (The unit measured for the flow threshold pressure is "bar").

**Table 7.** Start-up pressure threshold settings.

From Equil Region (I)	To Equil Region (J)	Threshold Pressure for Flow from I to J
1	2	170

Initiation of pressure gradient modelling for permeability velocity is as follows:

$$\left\{ \begin{array}{l} V = 0 \\ V = \frac{K}{\mu} \left( \frac{\Delta P}{L} - C \right) \end{array} \quad \left\{ \begin{array}{l} \frac{\Delta P}{L} < 0 \\ \frac{\Delta P}{L} \geq 0 \end{array} \right. \right\} \quad (14)$$

where  $V$  represents the seepage velocity, m/s;  $K$  represents the permeability of the reservoir matrix, mD;  $\mu$  corresponds to the viscosity of the crude oil, mPa·s;  $C$  represents the designated or proposed initiation of the pressure gradient, MPa/m; and  $\Delta P$  serves as the pressure differential between two points of distance  $L$  measurements on the grid, MPa.

According to the theory of limiting well spacing, the maximum flowing distance of the pressure gradient adopted should be greater than the starting pressure gradient, so the differential pressure  $\Delta P$  satisfies  $LC < \Delta P$ . For the study area, when the production differential pressure reaches 17 MPa, the maximum production range when considering the start-up pressure gradient is 400 m, which is realistic.

#### 4.2. Stress Sensitivity Analysis of Ultra-Deep Carbonate Reservoirs

According to the dual-porosity medium model that considers the initiation of pressure gradient and stress sensitivity, and includes formulas for both matrix and fracture stress sensitivity, we can see that in ultra-deep reservoirs consisting of fractured pore carbonate reservoirs, the degree of fracture permeability degradation in response to increased effective stress is more severe than the degradation seen in the matrix which is stress-sensitive, while showing a clear attenuation or decay characteristic. This effect is particularly pronounced near the bottom of the production wells, where the fracture permeability degradation is significantly greater than that seen in the matrix.

Take the T74 reservoir of the Yijiangfang formation in the research area as an example to perform statistical analysis on the fracture development, establish a fracture model in Petrel, and perform numerical simulation of the fracture using Tnavigator software.

Stress-sensitive settings in the simulator are as follows:

SATNUM = 1 (Matrix)	
PERMX	$ARRPERMX * E^{(-0.009324 * (1.465 - 0.324 \ln E) \Delta P)}$
PERMY	$ARRPERMY * E^{(-0.009324 * (1.465 - 0.324 \ln E) \Delta P)}$
PERMZ	$ARRPERMZ * E^{(-0.009324 * (1.465 - 0.324 \ln E) \Delta P)}$
SATNUM = 2 (Fractured)	
PERMX	$ARRPERMX * E^{(-0.125 * \Delta P / E)}$
PERMY	$ARRPERMY * E^{(-0.125 * \Delta P / E)}$
PERMZ	$ARRPERMZ * E^{(-0.125 * \Delta P / E)}$

During actual development, it was found that the stress sensitivity of the carbonate reservoir mainly occurs at the bottom of the well. Comparative changes in the initial and stress-sensitive permeability of matrix-type carbonate reservoirs in the 15th (bottom of the well) and 34th (The oil–water interface) layers are illustrated in Figures 8 and 9. For the entire matrix-type carbonate reservoir, a reduction of approximately 1.6% in permeability occurred at a Young’s modulus of 53.41 GPa. The lower rock stiffness may lead to fractures and plastic deformation that results in pore closure, and thus reduces the permeability of the rock (Figure 10).

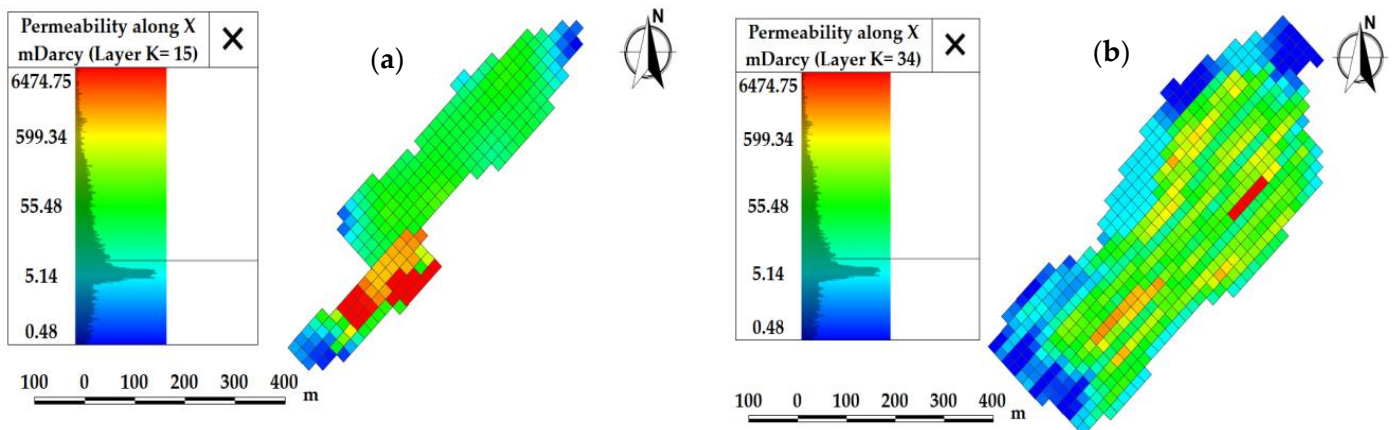


Figure 8. Initial permeability of matrix-type carbonate reservoirs. Layer (a) = 15; (b) = 34.

Figures 11 and 12 illustrate comparative changes in the initial and stress-sensitive permeability of fracture-type carbonate reservoirs in the 15th and 34th layers. For the entire fracture-type carbonate reservoir, the loss rate of permeability was approximately 65% at a Young’s modulus of 5.041 GPa. A lower Young’s modulus indicates higher elasticity and a greater tolerance to the corresponding deformation changes, but without significant fracture deformation (Figure 13). Therefore, in comparing the stress sensitivities between matrix-type carbonate reservoirs and fracture-type carbonate reservoirs, a higher stress

sensitivity has been observed for the case of fractured developments in carbonate reservoirs (Figure 14).

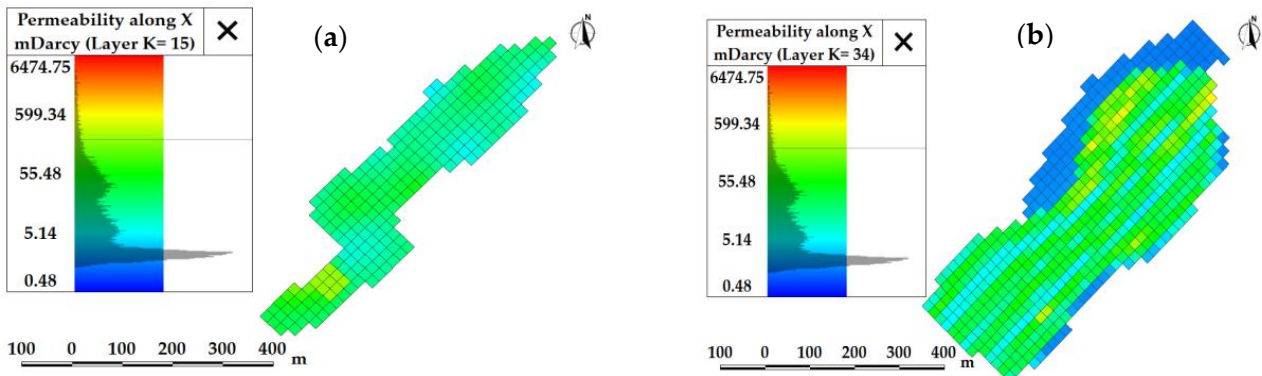


Figure 9. The permeability under the stress sensitivity impact in matrix-type carbonate reservoirs. Layer (a) = 15; (b) = 34.

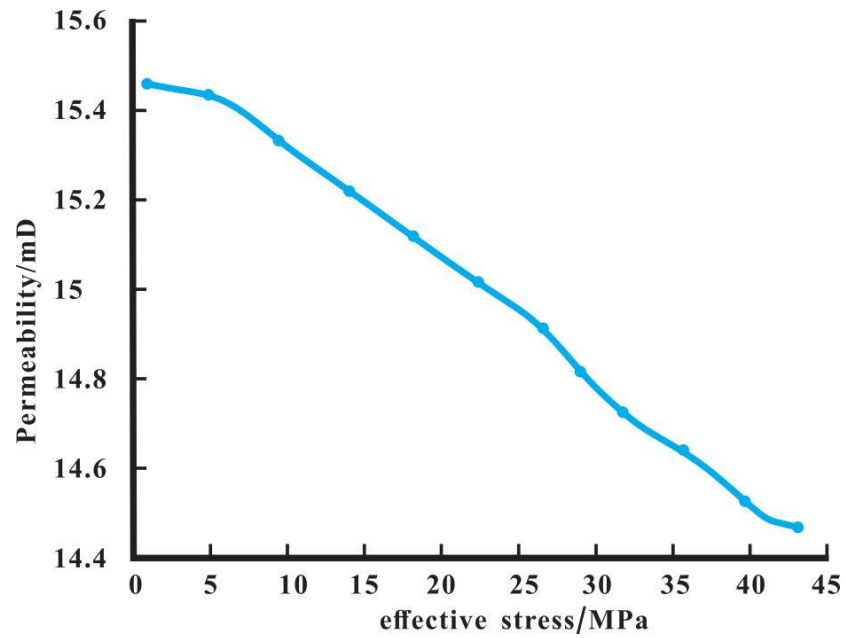


Figure 10. Permeability change curve of matrix-type carbonate reservoirs.

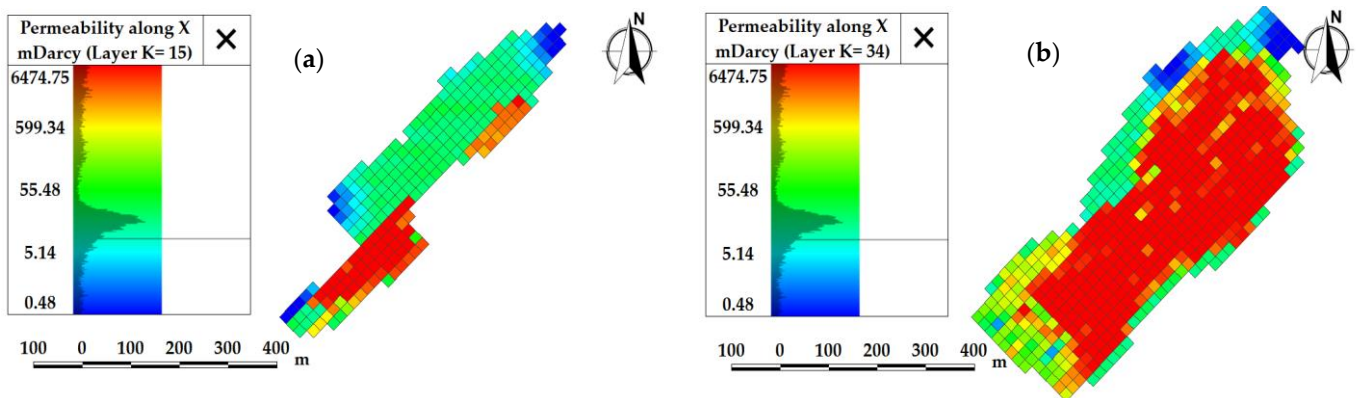
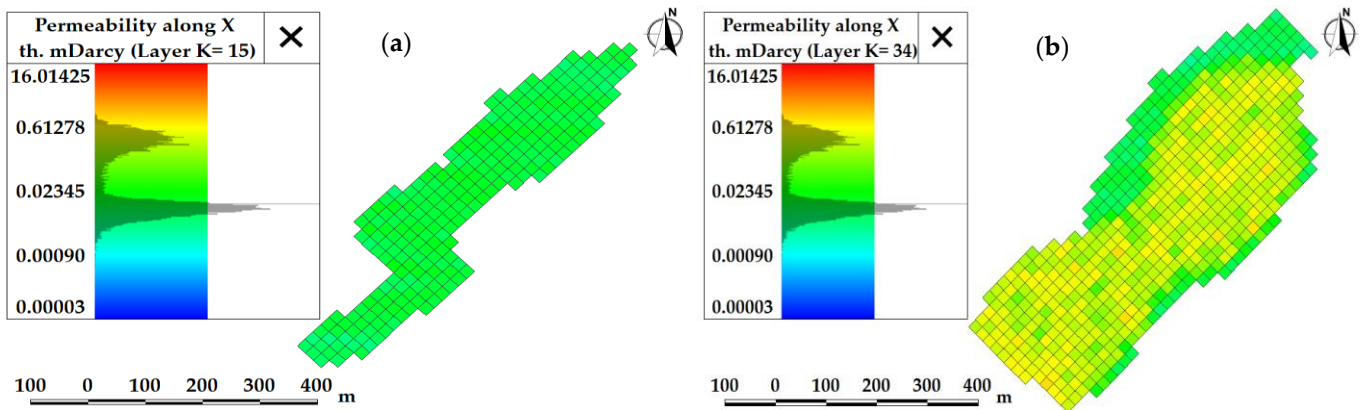
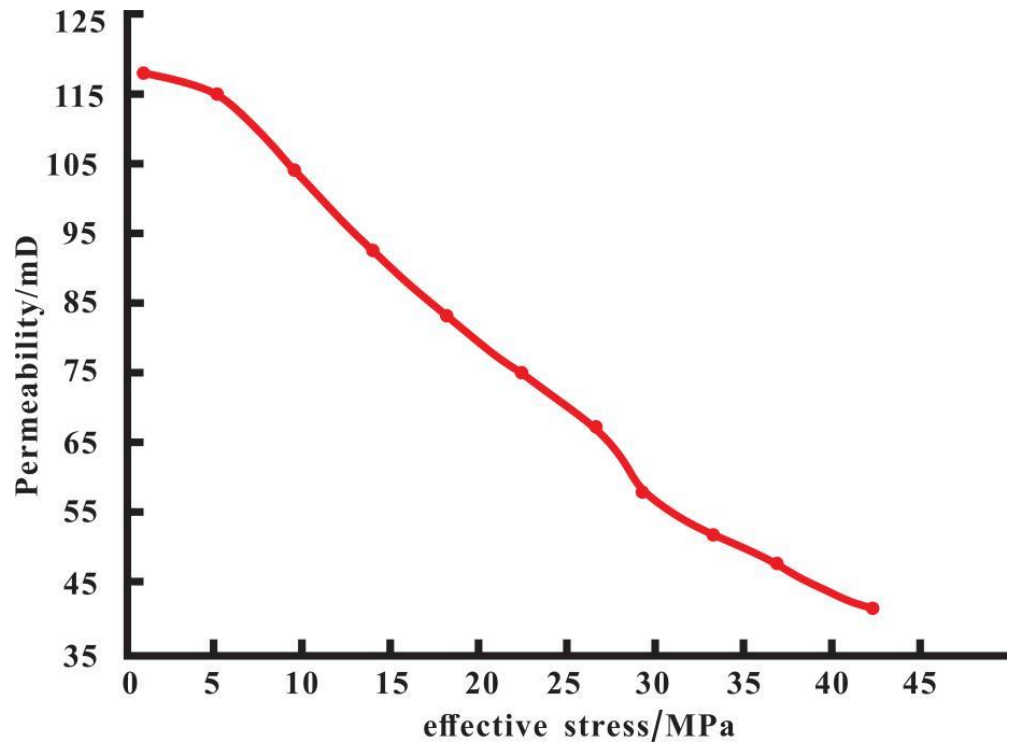


Figure 11. Initial permeability of fractured carbonate reservoirs. Layer (a) = 15; (b) = 34.



**Figure 12.** Permeability under the influence of stress sensitivity in fractured carbonate reservoirs. Layer (a) = 15; (b) = 34.



**Figure 13.** Permeability change curve of fractured carbonate reservoirs.

Through the analysis of the changing pressure and permeability of the reservoir’s overall area (Figure 15), it has been found that the influence of stress changes on the overall performance of the reservoir exhibits apparent spatial distribution characteristics. The stress sensitivity exhibited particular emphasis in the regions near the bottom of the well, which may be related to the distribution and connectivity of crack networks. These observations hold significant value towards optimizing drilling layout and improving the recovery rate.

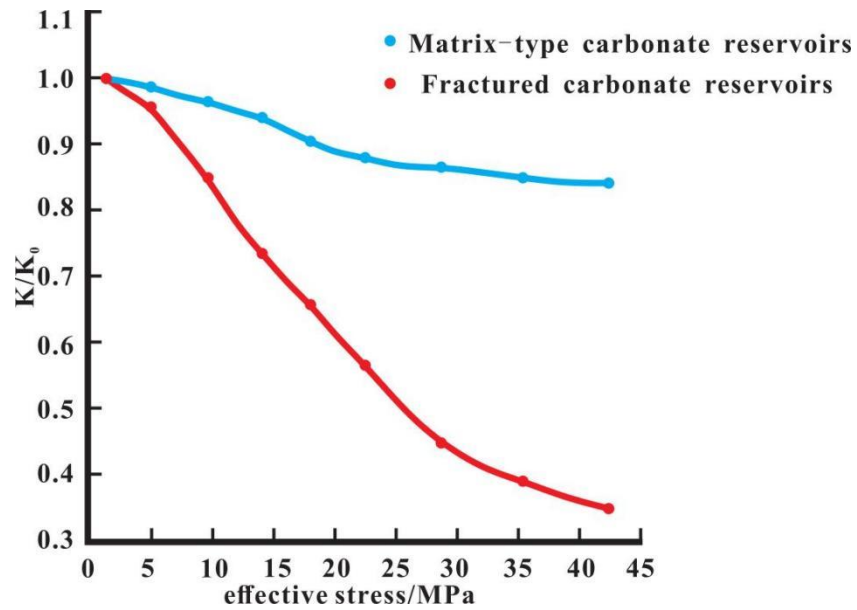


Figure 14. Comparison of stress sensitivity curves for matrix-type and fractured carbonates.

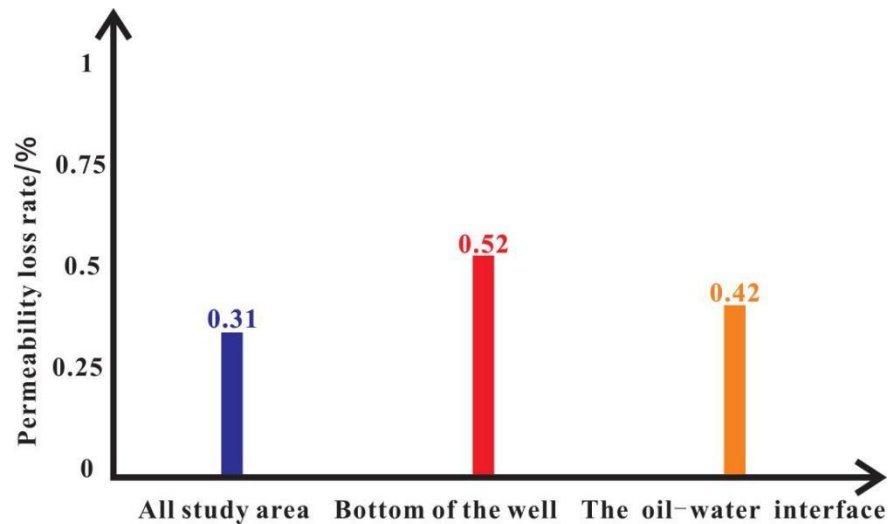


Figure 15. A comparison chart of the degree of permeability loss.

### 5. Discussion

This study combines experiments and numerical simulations to conduct an in-depth study of the stress sensitivity of ultra-deep carbonate reservoirs. Our results show that the stress sensitivity of matrix and fractured carbonate reservoirs is closely related to the Young’s modulus of the rock framework under the same effective stress conditions. This finding is consistent with the results of Jones, who found a linear relationship between the Young’s modulus of the rock and stress sensitivity. However, our study further reveals that under ultra-deep conditions, the stress sensitivity of fractured reservoirs is usually higher than that of matrix reservoirs, which may be related to the development and direction of the cracks. However, during our literature review process, we found that Du Shuheng [35] considered the aspect ratio of the length-to-width of cracks when studying the stress sensitivity of shale. We did not conduct a thorough investigation into this, and this is an aspect that we need to improve on.

When discussing our research results, we must consider the limitations of our methods. Although our experimental design aims to simulate realistic geological conditions, the selection of samples and experimental conditions may not fully capture the complexity

of ultra-deep carbonate reservoirs. For example, we did not simulate the influence of temperature changes on the rock mechanic properties in the experiments, which may play an important role in actual reservoirs. In addition, our numerical simulation may not fully consider all factors that affect changes in permeability, such as changes in fluid pressure and rock heterogeneity.

Compared with traditional methods of evaluating stress sensitivity, such as Pedrosa's flow equation solutions and Kikani's perturbation analysis, our research proposes a more intuitive and quantitative evaluation method. By establishing a dual-porosity media model, we can more accurately simulate and predict the changes in the permeability of reservoirs under different stress conditions. However, during the experimental stage, due to the limitations of actual core samples, we obtained relatively few cores, which may have caused accidental results in our experiments. In addition, when dealing with complex fracture reservoir networks, our models may need further testing and adjustment.

In practical applications, our research has important implications for the development of ultra-deep carbonate reservoirs. By accurately evaluating stress sensitivity, we may optimize drilling strategies, reduce permeability loss during production processes, and thus increase the efficiency of oil and gas field development. Future research can explore the stress sensitivity under different geological conditions and develop new experimental and simulation methods to improve the accuracy of evaluation.

Future research should be dedicated to overcoming the limitations of current research and further validating our results, for example, by improving the representativeness of the research by increasing the quantity and diversity of the samples. In addition, future research can explore the effects of temperature, chemical reactions, and changes in fluid pressure on stress sensitivity. Through these efforts, we can better understand the complex behavior of ultra-deep carbonate reservoirs, and provide a scientific basis for the effective development of oil and gas resources.

## 6. Conclusions

By fully considering the characteristics of carbonate reservoirs and exploring the mechanical properties of rocks, such as Young's modulus and Poisson's ratio, under different stress conditions, and through utilizing classic Griffith mechanics solutions, conventional Darcy's law, sedimentary structures, and layer sequence stratigraphic features, quantitative evaluation formulas for the stress sensitivity of matrix and fractured carbonate reservoirs were derived. These formulas were applied in the Shunbei area of the Tarim Basin and the following main conclusions were reached:

- (1) Under the same effective stress, the stress sensitivity of matrix- and fracture-type carbonate reservoirs is related to Young's modulus of the rock framework. In matrix-type carbonate reservoirs, rocks with a higher Young's modulus exhibit lower stiffness and are more susceptible to both elastic and plastic deformation, resulting in a higher level of stress sensitivity. Matrix-type carbonate reservoirs with a lower Young's modulus typically exhibit higher levels of stiffness, and thus may not readily undergo plastic deformation, resulting in a lower level of stress sensitivity. For the fracture-type carbonate reservoirs, those with a lower Young's modulus possess a higher resilience and capacity for elastic deformation, making them more likely to undergo fracture closure and less susceptible to significant deformation and stress sensitivity. When Young's modulus of fracture-type carbonate reservoirs is higher, the stiffness of the rock is large, making it easy for external stress changes to bring about the crack extension, resulting in a higher level of stress sensitivity.
- (2) Under a confining pressure of 87 MPa, a flow pressure of 50 MPa, and at 120 °C, it was determined that the effective stress of the matrix-type carbonate reservoir and the permeability of the reservoir exhibit an exponential relationship, with a stress sensitivity index  $\sigma$  of 0.009324. Based on rock mechanics parameters, with a matrix Young's modulus of 53.41 GPa and a Poisson's ratio of 0.201, and a fracture Young's modulus of 5.041 GPa and a Poisson's ratio of 0.33, the stress sensitivity of the fracture-

type carbonate reservoir is generally larger than that of the matrix-type carbonate reservoir, and the smaller the Young's modulus, the greater the difference in stress sensitivity between the two types of rocks.

- (3) By establishing a dual-porosity model based on the initiation pressure gradient, stress sensitivity simulations were conducted for typical ultra-deep carbonate formations in the Shunbei area of the Tarim Basin. The results indicated that these ultra-deep formations are characterized by high levels of stress sensitivity, providing new evidence for the high-stress sensitivity characteristics of ultra-deep carbonate reservoirs. The impact of stress sensitivity on the calculation of reserves and the efficient development of ultra-deep carbonate reservoirs must be given considerable attention during practical mining processes.

**Author Contributions:** Conceptualization, W.C. and S.J.; data curation, W.C.; formal analysis, S.J. and H.L.; funding acquisition, S.J.; methodology, W.C. and H.L.; project administration, H.L. and S.J.; software, W.C.; writing—original draft, W.C.; writing—review and editing, S.J. and H.L.; visualization, W.C.; validation, S.J. and H.L. All authors have read and agreed to the published version of the manuscript.

**Funding:** This research is funded by the Open Project of State Key Laboratory of Shale Oil and Gas Enrichment Mechanisms and Effective Development (GSYKY-B09-33).

**Institutional Review Board Statement:** Not applicable.

**Informed Consent Statement:** Not applicable.

**Data Availability Statement:** All data and materials are available on request from the corresponding author. The data are not publicly available due to ongoing research using a part of the data.

**Conflicts of Interest:** The authors declare no conflicts of interest.

## References

1. Guo, X. Breakthroughs in deep and ultra-deep oil and gas exploration and development in China driven by key core technology breakthroughs. *Energy* **2022**, *46*–50.
2. Chang, Q. New proven geological reserves of oil exceeded 1.6 billion tons last year. *Econ. Manag.* **2022**. [[CrossRef](#)]
3. Fan, J.; Li, F.; Hu, S.; Gao, K.; Xu, J. Larger diatoms are more sensitive to temperature changes and prone to succumb to warming stress. *Limnol. Oceanogr.* **2023**, *68*, 2512–2528. [[CrossRef](#)]
4. Li, Y.; Xue, Z.; Cheng, Z.; Jiang, H.; Wang, R. Progress and development directions of deep oil and gas exploration and development in China. *China Pet. Explor.* **2020**, *25*, 45–57.
5. Zhao, W.; Shen, A.; Qiao, Z.; Zhang, J.; Ni, X. Theoretical progress in carbonate reservoir and discovery of large marine oil and gas fields in China. *China Pet. Explor.* **2022**, *27*, 1–15.
6. Ehrenberg, S.N.; Nadeau, P.H. Sandstone vs. carbonate petroleum reservoirs: A global perspective on porosity-depth and porosity-permeability relationships. *AAPG Bull.* **2005**, *89*, 435–445. [[CrossRef](#)]
7. Martyushev, D.A.; Davoodi, S.; Kadkhodaie, A.; Riazi, M.; Kazemzadeh, Y.; Ma, T. Multiscale and diverse spatial heterogeneity analysis of void structures in reef carbonate reservoirs. *Geoenergy Sci. Eng.* **2024**, *233*, 212569. [[CrossRef](#)]
8. Khan, N. Carbonate facies patterns of the Lutetian-Priabonian strata from the western Indian plate margin: Reservoir potential and palaeoclimatic implications. *Mar. Pet. Geol.* **2023**, *154*, 106313. [[CrossRef](#)]
9. Liu, F.; Wang, Y.; Chen, X.; Su, Y.; Wang, Y. Analysis on oil well productivity of low-permeability reservoirs with stress sensitivity being taken into consideration. *Oil Gas Geol.* **2013**, *34*, 124–128.
10. Sun, K.; Liu, H.; Wang, J.; Liu, R.; Feng, Y.; Kang, Z.; Zhang, Y. Stress sensitivity characteristics of deep carbonate fractured porous media. *Geol. Front.* **2023**, *30*, 351–364. [[CrossRef](#)]
11. Chen, X.; Shen, X.; Liu, J.; Shen, G. Distribution of natural fractures and mechanical characteristics of orogenic movement carbonate formations in Shunbei Oilfield. *Xinjiang Pet. Geol.* **2021**, *42*, 515–520.
12. Jones, F. A laboratory study of effects of confining pressure on fracture flow and storage capacity in carbonate rocks. *J. Pet. Technol.* **1975**, *27*, 21–27. [[CrossRef](#)]
13. Pedrosa, O. Pressure Transient Response in Stress-Sensitive Formations. In Proceedings of the SPE California Regional Meeting, Oakland, CA, USA, 2–4 April 1986. [[CrossRef](#)]
14. Kikani, J.; Pedrosa, O.A., Jr. Perturbation Analysis of Stress-Sensitive Reservoirs. *SPE Form. Eval.* **1991**, *6*, 379. [[CrossRef](#)]
15. Tong, D.; Zhang, H. Flow analysis of fluid in fractal reservoir with deformed double-porosity medium. *J. Pet. Univ. Nat. Sci. Ed.* **2003**, *27*, 76–79+151.
16. Li, C. Evaluation method for stress sensitivity of reservoir rocks. *Daqing Pet. Geol. Dev.* **2006**, *40*–42+105.

17. Fernandes, F.B.; Braga, A.M.B.; de Souza, A.L.S.; Soares, A.C. Mechanical formation damage control in permeability Biot's effective stress-sensitive oil reservoirs with source/sink term. *J. Pet. Sci. Eng.* **2023**, *220*, 111180. [[CrossRef](#)]
18. Shovkun, I.; Espinoza, D.N. Coupled fluid flow-geomechanics simulation in stress-sensitive coal and shale reservoirs: Impact of desorption-induced stresses, shear failure, and fines migration. *Fuel* **2017**, *195*, 260–272. [[CrossRef](#)]
19. Cheng, Y.; Guo, C.; Chen, P.; Shi, H.; Tan, C. Stress sensitive of carbonate gas reservoirs and its microscopic mechanism. *Pet. Explor. Dev.* **2023**, *50*, 152–159. [[CrossRef](#)]
20. Moradi, M.; Shamloo, A.; Asadbegi, M.; Dezfuli, A.D. Three dimensional pressure transient behavior study in stress sensitive reservoirs. *J. Pet. Sci. Eng.* **2017**, *152*, 204–211. [[CrossRef](#)]
21. Das, A.K. Generalised Darcy's law with source implications. *Xinjiang Pet. Sci. Technol. Inf.* **1999**, *20*, 73–77.
22. Li, S.; Ren, L.; Zhen, P.; Gui, Q. Similar Structure of the Solution to the Dual-Porosity Model for Naturally Fractured Shale Gas Reservoirs Based on Stress Sensitivity. *Appl. Math. Mech.* **2017**, *38*, 233–242.
23. Hajiabdolmajid, V.; Kaiser, P.K.; Martin, C.D. Modelling brittle failure of rock. *Int. J. Rock Mech. Min. Sci.* **2002**, *39*, 731–741. [[CrossRef](#)]
24. Parastatidis, E.; Hildyard, M.W.; Nowacki, A.; Flynn, W.J.; Suikkanen, J. Excavation Damage Zone fracture modelling for seismic tomography: A comparison of explicit fractures and effective medium approaches. *Int. J. Rock Mech. Min. Sci.* **2023**, *170*, 105509. [[CrossRef](#)]
25. Roşu, A.M.; Severin, F.; Roşu, O.C.; Cobzeanu, B.M.; Gherasimescu, S.; Sava, F.P.; Palade, D.O.; Drochioi, C.I.; Costan, V.V.; Cobzeanu, M.D. Patterns and Characteristics of Midface Fractures in North-Eastern Romania. *Medicina* **2023**, *59*, 510. [[CrossRef](#)] [[PubMed](#)]
26. Bernabe, Y. An effective pressure law for permeability in chelmsford granite and barre granite. *Int. J. Rock Mech. Min. Sci. Geomech. Abstr.* **1986**, *23*, 267–275. [[CrossRef](#)]
27. Zhao, J.; Xiao, W.; Li, M.; Xiang, Z.; Li, L.; Wang, J. The effective pressure law for permeability of clay-rich sandstones. *Pet. Sci.* **2011**, *8*, 194–199. [[CrossRef](#)]
28. Taheri, K.; Alizadeh, H.; Askari, R.; Kadkhodaie, A.; Hosseini, S. Quantifying fracture density within the Asmari reservoir: An integrated analysis of borehole images, cores, and mud loss data to assess fracture-induced effects on oil production in the Southwestern Iranian Region. *Carbonates Evaporites* **2024**, *39*, 8. [[CrossRef](#)]
29. Siddhamshetty, P.; Bhandakkar, P.; Kwon, J.S.I. Enhancing total fracture surface area in naturally fractured unconventional reservoirs via model predictive control. *J. Pet. Sci. Eng.* **2020**, *184*, 106525. [[CrossRef](#)]
30. Taleghani, A.D.; Gonzalez, M.; Shojaei, A. Overview of numerical models for interactions between hydraulic fractures and natural fractures: Challenges and limitations. *Comput. Geotech.* **2016**, *71*, 361–368. [[CrossRef](#)]
31. Li, Z.; Wang, Q. Methods and technique for prediction of ultra-deep carbonate reservoirs in north Tarim Basin. *Oil Gas Geol.* **2002**, 35–40+44.
32. Ma, Y.; Cai, X.; Yun, L.; Li, Z.; Li, H.; Deng, S.; Zhao, P. Practice and theoretical and technical progress in exploration and development of Shunbei ultra-deep carbonate oil and gas fields, Tarim Basin, NW China. *Pet. Explor. Dev.* **2022**, *49*, 1–20. [[CrossRef](#)]
33. Gu, R.; Yun, L.; Zhu, X.; Zhu, M. Oil and gas sources in Shunbei Oilfield, Tarim Basin. *Pet. Exp. Geol.* **2020**, *42*, 248–254+262.
34. Ji, B.; Zheng, S.; Gu, H. On the development technology of fractured-vuggy carbonate reservoirs: A case study on Tahe oilfield and Shunbei oil and gas field. *Oil Gas Geol.* **2022**, *43*, 1459–1465.
35. Du, S.; Shen, W.; Zhao, Y. Quantitative evaluation of stress sensitivity in shale reservoir: Ideas and applications. *J. Mech.* **2022**, *54*, 2235–2247.

**Disclaimer/Publisher's Note:** The statements, opinions and data contained in all publications are solely those of the individual author(s) and contributor(s) and not of MDPI and/or the editor(s). MDPI and/or the editor(s) disclaim responsibility for any injury to people or property resulting from any ideas, methods, instructions or products referred to in the content.